

NICKEL-GADOLINIUM PHASE DIAGRAM

By M. I. Copeland, M. Krug, C. E. Armantrout,
and H. Kato

* * * * * report of investigations 6566



UNITED STATES DEPARTMENT OF THE INTERIOR
Stewart L. Udall, Secretary

BUREAU OF MINES
Marling J. Ankeny, Director

DISTRIBUTION OF THIS DOCUMENT IS UNLIMITED

REA

DISCLAIMER

This report was prepared as an account of work sponsored by an agency of the United States Government. Neither the United States Government nor any agency Thereof, nor any of their employees, makes any warranty, express or implied, or assumes any legal liability or responsibility for the accuracy, completeness, or usefulness of any information, apparatus, product, or process disclosed, or represents that its use would not infringe privately owned rights. Reference herein to any specific commercial product, process, or service by trade name, trademark, manufacturer, or otherwise does not necessarily constitute or imply its endorsement, recommendation, or favoring by the United States Government or any agency thereof. The views and opinions of authors expressed herein do not necessarily state or reflect those of the United States Government or any agency thereof.

DISCLAIMER

Portions of this document may be illegible in electronic image products. Images are produced from the best available original document.

This publication has been cataloged as follows:

Copeland, Mark I

Nickel-gadolinium phase diagram, by M. I. Copeland [and others. Washington] U. S. Dept. of the Interior, Bureau of Mines [1964]

24 p. illus., tables. (U. S. Bureau of Mines. Report of investigations 6566)

Includes bibliography.

1. Nickel alloys. 2. Gadolinium alloys. 3. Phase rule and equilibrium. I. Title. (Series)

TN23.U7 no. 6566 622.06173

U. S. Dept. of the Int. Library

CONTENTS

	<u>Page</u>
Abstract.....	1
Introduction.....	1
Experimental procedures and results.....	3
Materials and melting procedure.....	3
Annealing treatment and hardness of alloys.....	4
Phase diagrams.....	5
Melting-point determinations.....	6
Heat treatments and metallography.....	7
Phases observed.....	9
X-ray diffraction data.....	9
Discussion of results.....	17
Conclusions.....	22
References.....	23

ILLUSTRATIONS

Fig.

1. Nickel-gadolinium phase diagram.....	5
2. Nickel-gadolinium phase diagram, metallography, and thermal data...	6
3. Structure of the intermetallic compound $Ni_{15}Gd_2$	9
4. Dendritic structure observed in an Ni-10 wt pct Gd alloy.....	18
5. Cored structure in Ni-26.4 wt pct Gd specimen developed after heat treatment at $1,310^{\circ}C$	18
6. Structure of an Ni-37.5 wt pct Gd alloy held at $10^{\circ}C$ above the peritectic isotherm occurring at $1,270^{\circ}C$	19
7. Cored structure in an Ni-45 wt pct Gd alloy after heat treatment at $10^{\circ}C$ above the peritectic isotherm occurring at $1,180^{\circ}C$	19
8. Cored structure observed after holding at $10^{\circ}C$ above the peritectic isotherm at $1,070^{\circ}C$, where Ni_2Gd melted incongruently.....	20
9. Eutectic structure observed in an Ni-70 wt pct Gd specimen held at $10^{\circ}C$ above the $890^{\circ}C$ isotherm.....	20
10. Duplex structure consisting of Ni_5Gd and Ni_7Gd_2 observed in an annealed Ni-39 wt pct Gd specimen.....	21
11. $NiGd$ and $NiGd_3$ phases observed in an Ni-80 wt pct Gd alloy.....	21

TABLES

1. Selected properties of nickel and gadolinium.....	3
2. Impurity analyses of nickel and gadolinium.....	3
3. Analysis and hardness of alloys.....	4
4. Liquidus and solidus data.....	8
5. $Ni_{15}Gd_2$ X-ray diffraction data.....	11
6. Ni_5Gd X-ray diffraction data.....	12
7. Ni_7Gd_2 X-ray diffraction data.....	13
8. Ni_3Gd X-ray diffraction data.....	14
9. Ni_2Gd X-ray diffraction data.....	15
10. $NiGd$ X-ray diffraction data.....	16
11. $NiGd_3$ X-ray diffraction data.....	17

NICKEL-GADOLINIUM PHASE DIAGRAM

by

M. I. Copeland,¹ M. Krug,² C. E. Armantrout,³ and H. Kato³

ABSTRACT

The investigation of the nickel-gadolinium phase diagram was undertaken to determine the alloying behavior of these two metals. The data from melting-point determinations, thermal analyses, metallographic examinations, and X-ray diffraction analyses revealed a phase diagram with three eutectic points and seven intermetallic compounds. Very limited solubility of the phases in each other was observed. The five phases, $\text{Ni}_{15}\text{Gd}_2$, Ni_7Gd_2 , Ni_3Gd , Ni_2Gd , and NiGd_3 , melted incongruently at about 1,300°, 1,270°, 1,180°, 1,070°, and 775° C, respectively. Ni_5Gd and NiGd melted congruently at approximately 1,550° and 980° C, respectively. Four of the compounds were determined to crystallize in the hexagonal system: $\text{Ni}_{15}\text{Gd}_2$, Ni_5Gd , Ni_7Gd_2 , and Ni_3Gd . Ni_2Gd was determined to be cubic and NiGd , orthorhombic. The crystal system of NiGd_3 was not determined. The eutectic points occurred at 13, 67, and 85 wt pct gadolinium, and the isotherms at 1,290°, 890°, and 700° C, respectively.

INTRODUCTION

Because of their high thermal neutron capture cross section, the possible utilization of a number of rare-earth elements as control rod materials in power-producing atomic reactors has been considered by the Atomic Energy Commission. However, the rare-earth metals of interest are very reactive, and they must be protected from corrosive environments or be made corrosive resistant.

The search for new corrosion-resistant alloys for application in the atomic energy field prompted the investigation of the stainless steel-gadolinium phase diagram by the Bureau of Mines. Gadolinium was one of the

¹Physical metallurgist (research).

²Physicist (general).

³Supervising physical metallurgist.

All authors are with the Albany Metallurgy Research Center, Bureau of Mines, Albany, Oreg.

rare-earth elements of special interest because of its high thermal neutron capture cross section, about 46,000 barns (13).⁴ Previous work conducted by the Bureau indicated that gadolinium could be easily alloyed with AISI type 304 stainless steel, extra low carbon. This type of stainless steel has a nominal composition of 18 wt pct chromium, 8 wt pct nickel, and 74 wt pct iron.

Shortly after the investigation of the stainless steel-gadolinium phase diagram was initiated, it became obvious that the identification of the multitude of phases observed was impossible with the data available. As many as four unknown phases in one alloy composition were observed. It soon became apparent that the identification of the phases in this multicomponent alloy would have to be based in part on data from the investigation of the binary alloys, Fe-Gd, Cr-Gd, and Ni-Gd. The investigation of the Fe-Gd alloy system was completed and reported by the Bureau of Mines (4). The chromium-gadolinium system was reported by the senior author at the Second Rare Earth Conference (3) as a part of the Bureau's research effort. The Ni-Gd phase diagram investigation is presented in this report. The phase diagrams of the other possible binary alloys, Fe-Cr, Cr-Ni, and Fe-Ni, have been thoroughly investigated and reported in the literature (11).

A search of the literature revealed the existence of several compounds in the nickel-gadolinium alloy system. Endter and Klemm (8) reported the compound Ni_5Gd which is isotypic with Cu_5Ca . Wernick and Geller (20) prepared rare earth-nickel compounds with MgCu_2 -type structure, one of which was Ni_2Gd . Moriarty and Baenziger (15) reported that Ni_5Gd , Ni_2Gd , NiGd_3 , and possibly Ni_7Gd_2 , Ni_4Gd , and Ni_3Gd exist in that alloy system. There were no references to metallographic studies of nickel-gadolinium alloys.

Table 1 lists selected physical properties of nickel and gadolinium, a few of which were useful in constructing and evaluating nickel-gadolinium phase diagrams. The physical properties of nickel are well established, but only recently were the properties of gadolinium accurately determined and reported in the literature (12).

A review of the theories of alloying indicated little possibility of significant terminal solid solubility in the nickel-gadolinium phase diagram. The Hume-Rothery (14) rule predicts only limited solubility when the atomic sizes differ by more than 15 percent. The disparity of atomic radii of nickel, 1.245 Å, and gadolinium, 1.802 Å, is greater than 15 percent. According to Gschneidner (10), electronegativity also is important in determining solid solubility. In general, a difference of electronegativities greater than 0.4 between two alloying elements is the limiting value at which any terminal solid solubility can be expected. The difference between the electronegativities of nickel, 1.80, and gadolinium, 1.20, is greater than 0.4.

⁴Underlined numbers in parentheses refer to items in the list of references at the end of this report.

TABLE 1. - Selected properties of nickel and gadolinium

Property	Nickel (18)	Gadolinium (12)
Atomic number.....	28.....	64.
Atomic weight.....	58.71.....	157.26.
Density at 20° C.....g/cm ³	8.902.....	7.92.
Melting point.....° C	1,453.....	1,312 ± 15.
Boiling point.....° C	2,730.....	2,830.
Atomic radius.....A	1.245.....	1.802.
Electronegativity (19).....	1.80.....	1.20.
Crystal structure.....	Face-centered cubic	Hexagonal close-packed. ¹
a ₀A	3.52.....	3.636.
c ₀A	5.783.
Thermal neutron capture cross section (13).....barns/atom	4.6 ± 0.2.....	46,000 ± 2,000.

¹Up to 1,264° C.

EXPERIMENTAL PROCEDURES AND RESULTS

Materials and Melting Procedure

Gadolinium and nickel of 99+ percent purity were used in this investigation. Analyses for impurity content of both metals are presented in table 2. The presence of elements other than those listed was not detected.

TABLE 2. - Impurity analyses of nickel and gadolinium

Impurity element	Nickel, ppm	Gadolinium, ppm
Chromium.....	(¹)	10- 100
Copper.....	>10	10- 100
Hydrogen.....	3	86
Iron.....	100-1,000	100-1,000
Magnesium.....	>10	10- 100
Manganese.....	(¹)	10- 100
Nickel.....	(²)	100-1,000
Nitrogen.....	10	280
Oxygen.....	115	1,875
Silicon.....	10- 100	10- 100
Titanium.....	100-1,000	(¹)
Tungsten.....	100-1,000	(¹)

¹Not detected.²No analysis.

The alloy charges were melted in a nonconsumable tungsten electrode arc furnace on a water-cooled copper hearth. The furnace atmosphere was controlled by evacuating, backfilling with helium, and gettering with gadolinium. Proportioned charges of 40 to 50 grams were melted four times or more with inverting between each melt to promote homogeneity in the alloys. The nominal composition of a number of alloys and the X-ray fluorescent analyses after

melting are tabulated in table 3. Chemical analyses mentioned in this report are in percent by weight unless otherwise specified.

TABLE 3. - Analysis and hardness of alloys

Composition, wt pct gadolinium		Knoop hardness		Annealing heat treatment
Nominal	Fluorescent analyses	As-cast	Annealed	
1.0	(¹)	(¹)	113	1,000° C, 3 days, furnace cooled.
5.0	4.9	143	153	Do.
10.0	(¹)	281	157	Do.
15.0	14.5	390	356	Do.
20.0	21.7	504	498	Do.
24.0	(¹)	632	608	Do.
27.5	26.7	726	577	Do.
30.0	30.7	(¹)	624	Do.
35.0	35.0	747	650	Do.
40.0	40.8	577	475	Do.
43.3	43.5	577	535	Do.
45.0	45.0	529	498	1,000° C, 2 days, furnace cooled.
50.0	50.0	434	542	Do.
55.0	55.0	529	522	Do.
57.2	57.3	(¹)	549	600° C, 2 weeks, furnace cooled.
60.0	(¹)	454	470	Do.
65.0	62.5	430	(¹)	Do.
70.0	(¹)	237	374	Do.
72.8	73.3	(¹)	258	Do.
75.0	(¹)	228	237	Do.
80.0	78.7	308	(¹)	Do.
85.0	85.0	251	262	Do.
89.0	88.3	(¹)	(¹)	Do.
90.0	90.0	237	535	Do.
95.0	(¹)	157	134	Do.
99.0	(¹)	119	64	Do.

¹ Not run.

Homogeneous and coherent ingot buttons were difficult to obtain on all alloys whose composition contained large amounts of intermetallic compounds. Most of the buttons were made homogeneous by repeated melting of the alloys. However, a slight difference in composition between the top and bottom was observed in a few buttons. A small degree of inhomogeneity could be expected because of the rapidity at which the copper hearth cools the buttons. Coherent buttons were difficult to obtain on the majority of the alloys with high compound composition. Shattering of the buttons was frequently noted on striking an arc to them on melting, and at times on cooling.

Annealing Treatment and Hardness of Alloys

After removing a sample from each ingot button for metallographic examination and before proceeding further with the investigation, the as-cast

nickel-gadolinium alloys were annealed. Most of the nickel-gadolinium alloys were very hard and brittle, and therefore they were not amenable to any hot- or cold-working procedure for homogenization or shaping procedures. The samples were annealed by heating in a tube furnace in a vacuum of 2.5×10^{-5} torr and allowing the furnace to cool. A molybdenum boat was used to hold the specimen and prevent reaction between the samples and the ceramic. The annealing heat treatments and the hardness of a few alloys before and after annealing are tabulated in table 3.

Phase Diagrams

The phase diagram was determined from data obtained by conducting melting-point, thermal analysis, heat treatment, metallographic examination, and X-ray diffraction analysis tests. Metallographic data were used as the final criterion. On the basis of the data obtained, the phase diagram as constructed is presented in figure 1. In figure 2, the majority of the metallographic and melting-point data are presented in the phase diagram.

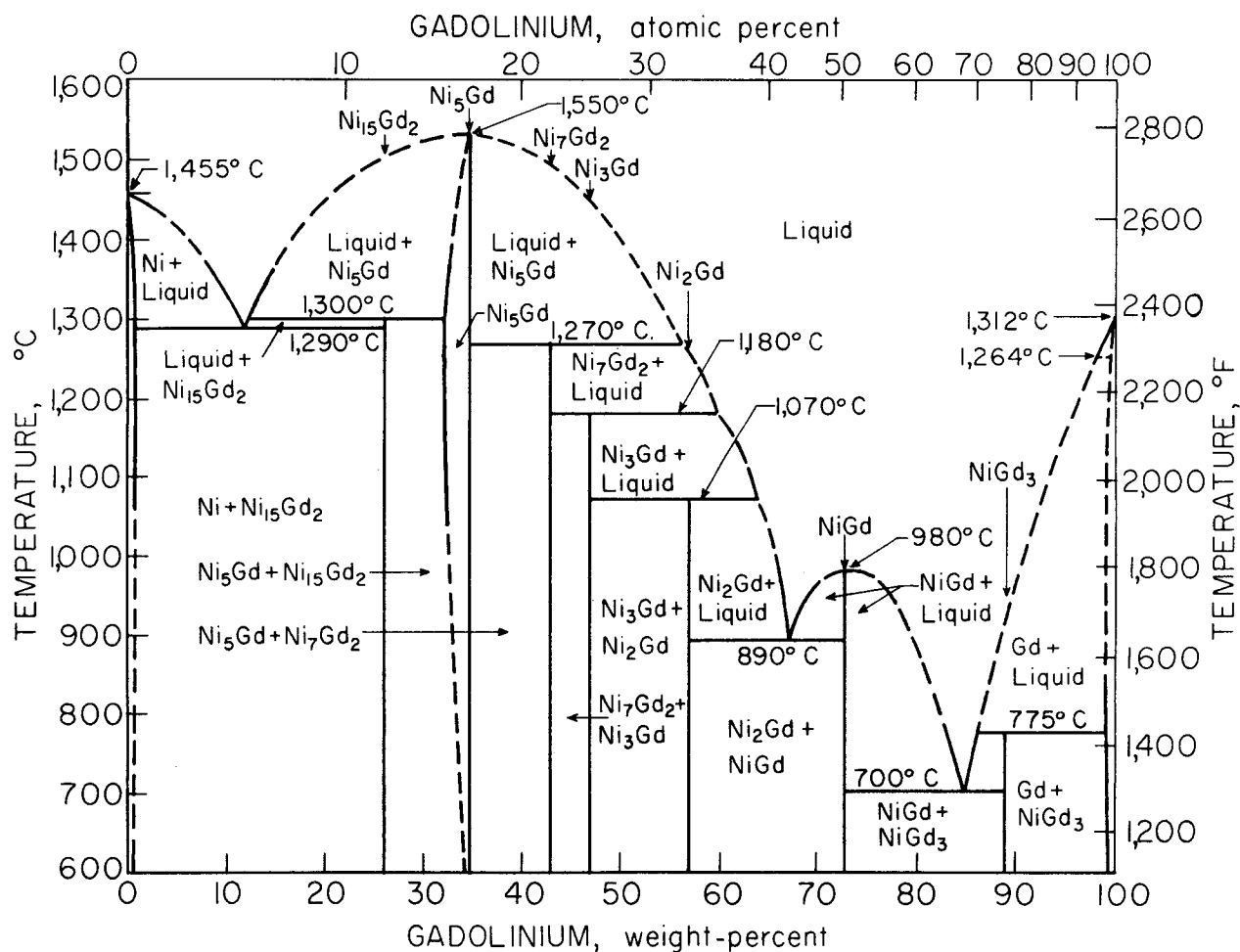


FIGURE 1. - Nickel-Gadolinium Phase Diagram.

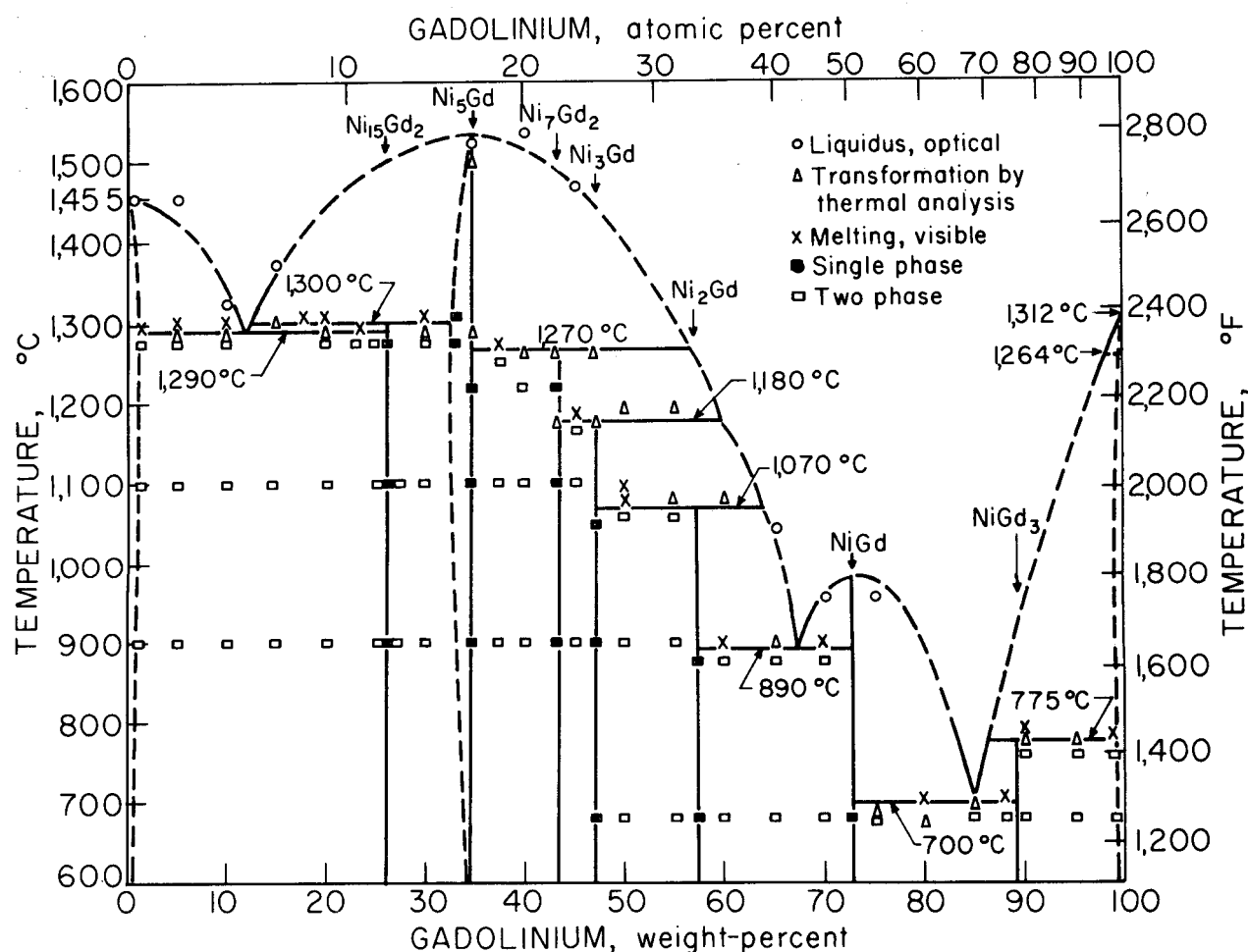


FIGURE 2. - Nickel-Gadolinium Phase Diagram, Metallography, and Thermal Data.

Melting-Point Determinations

Solidus and liquidus determinations were made using an optical pyrometer method and by thermal analyses. The optical pyrometer method was conducted according to the thermal gradient technique suggested by Deardorff and Hayes (7). A small cylindrical hole was drilled in the alloy sample, the specimen placed on a nickel pedestal, and heated at a relatively constant rate. The bottom of the hole was observed with a disappearing filament optical pyrometer, and the solidus was determined when a small droplet was observed in the bottom of the hole. The liquidus was determined as the temperature at which the hole was completely filled with liquid. All the optical melting-point determinations were conducted in a vacuum of 10^{-3} torr or less. The specimens were heated in an induction furnace which used a tantalum susceptor as a heat source. The data were useful in determining the melting points of the two compounds that melted congruently (Ni_5Gd and NiGd) and obtaining generalized information on the eutectic isotherms and peritectic reaction isotherms for the remaining compounds. The data were not believed

to be adequate for accurately placing the isotherm at which the compounds ($\text{Ni}_{15}\text{Gd}_2$, Ni_7Gd_2 , Ni_3Gd , Ni_2Gd , and NiGd_3) melted peritectically, nor when the alloy composition was not close to the eutectic point.

Thermal analyses were conducted by both differential and time-temperature techniques. Using differential thermal analysis, one insulated Chromel-Alumel⁵ thermocouple was inserted in a hole drilled in the specimen under investigation and another in a hole drilled in a neutral body, molybdenum. A three-wire system was used. One lead wire from each thermocouple to the outside of the furnace was alumel. The common lead wire between the thermocouples was chromel from which a wire of the same material to the outside of the furnace was made. The entire assembly was placed in a tube, evacuated to 2.0×10^{-5} torr, and heated by a resistance furnace at about 5°C per minute. The emf (millivoltage) across the Chromel-Alumel thermocouple in the specimen was used to determine the temperature and the emf across the Alumel wires to detect any temperature arrests. The changes in apparent heating or cooling rate were used to determine solidus and liquidus temperatures during differential thermal analysis. In the time-temperature method, the specimens were wrapped in a piece of tantalum foil, a tungsten-tungsten 26-percent rhenium thermocouple was spotwelded to the outside of the foil, and the whole assembly was then thermally cycled, using as uniform a heating and cooling rate in an induction furnace as possible. The endothermic reaction that occurs when metals go from the solid to the liquid state causes a decrease in the apparent rate of heating, and therefore may be taken as the solidus temperature. A vacuum of 10^{-3} torr or less was employed in the induction furnace.

Results from the solidus and liquidus determinations are listed in table 4, and a number of these are illustrated graphically in figure 2. These data indicated the presence of eight isotherms at $1,290^\circ$, $1,300^\circ$, $1,270^\circ$, $1,180^\circ$, $1,070^\circ$, 890° , 700° , and 775°C . Maxima in the liquidus were noted at $1,550^\circ$ and 980°C , where the compounds Ni_5Gd and NiGd melted congruently, respectively. Minima in the liquidus were observed at $1,290^\circ$, 890° , and 700°C where eutectic reactions occurred. Peritectic reactions occurred at the remaining isotherms.

Heat Treatments and Metallography

An extensive amount of metallographic work was conducted for the following reasons on this system: first, to check the homogeneity and to determine structures in as-cast alloys; second, to determine the effect of annealing on obtaining homogenized structures and to determine the phases present; and third, to determine the effectiveness of each heat treatment by observing phases present.

⁵References to trade or brand names are made only for identification and mention of them does not imply endorsement by the Bureau of Mines.

TABLE 4. - Liquidus and solidus data

Composition, wt pct Gd	Optical method		Thermal analysis, solidus, ° C
	Liquidus, ° C	Solidus, ° C	
0	1,455	1,455	(¹)
5	1,460	1,380	1,290
10	1,330	1,290	1,290
15	1,375	1,255	1,300
20	1,370	1,250	1,290
25	1,410	1,260	(¹)
30	1,415	1,265	1,290
35	1,540	1,380	1,283, 1,500
37.5	(¹)	(¹)	1,260
40	1,550	1,310	1,274
43.3	(¹)	(¹)	1,263, 1,174
45	1,475	1,155	1,245, 1,163
47.1	(¹)	(¹)	1,263, 1,172
50	1,155	1,090	1,080, 1,195
55	1,155	1,090	1,080, 1,190
60	1,075	1,035	900, 1,080
65	1,045	1,045	890
70	960	(²)	890
75	955	(²)	894
80	(²)	(²)	675
85	(²)	(²)	697
90	(²)	(²)	775
95	(²)	(²)	768

¹No determination.²Not detected.

Specimens to be heat treated and cooled rapidly prior to examination by metallographic techniques were wrapped in molybdenum or tantalum foil and sealed in quartz ampules which were evacuated and partially backfilled with helium. The specimens were wrapped in the foil to prevent any reaction between the ampules and the specimen. The specimens were heat treated at 650° to 1,340° C from $\frac{1}{2}$ to 148 hours. The ampules containing the specimen were transferred from the furnace to water and fractured as rapidly as possible.

The heat-treated specimens were mounted in Bakelite and polished. Water was used as a coolant and lubricant in all but the last two polishing steps where diamond abrasive and kerosine were used. Three types of etchants were employed: 10 percent by weight chromic acid in water, 10 percent by weight oxalic acid in water, and nital etchants (1 to 5 percent by volume of HNO₃ in ethyl alcohol). The chromic and oxalic acid solutions were used to etch the specimens by electrolytic methods, using about 3 volts dc. Chromic acid solutions were used on alloys containing 1- to 26-percent gadolinium, and oxalic acid on alloys containing about 43 to 47 percent gadolinium. Nital was used on all the other alloys by swabbing the solution on the polished specimen and rinsing with absolute alcohol.

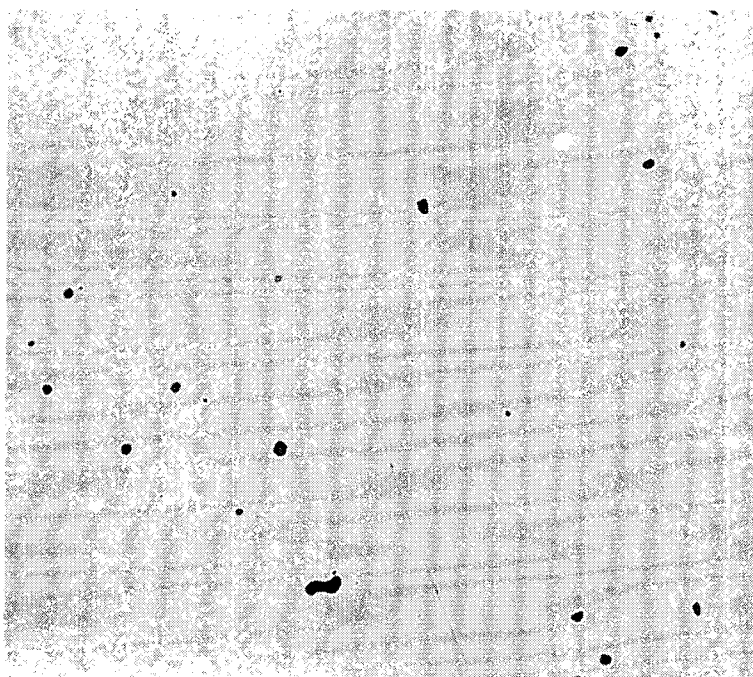


FIGURE 3. - Structure of the Inter-metallic Compound $\text{Ni}_{15}\text{Gd}_2$. (X 500); Nital Etch.

Phases Observed

Seven compounds were observed in the nickel-gadolinium alloy system. Five of these, $\text{Ni}_{15}\text{Gd}_2$, Ni_7Gd_2 , Ni_3Gd , Ni_2Gd , and NiGd_3 , melted incongruently as peritectic reactions at $1,300^\circ$, $1,270^\circ$, $1,180^\circ$, $1,070^\circ$, and 775° C, respectively. The two compounds, Ni_5Gd and NiGd , melted congruently at about $1,550^\circ$ and 980° C, respectively. With the exception of Ni_5Gd , all of the phases were observed to be intermetallic compounds of constant stoichiometric composition. A slight solid solubility of $\text{Ni}_{15}\text{Gd}_2$ in Ni_5Gd was noted.

Metallographic data observed after heat treatment are plotted in figure 2. Considerably more metallographic data were obtained in the course of the investigation, but for clarity these were left off the diagram. One of the phases, $\text{Ni}_{15}\text{Gd}_2$, observed in an alloy containing 26.4-wt pct gadolinium, is clearly illustrated in the photomicrograph illustrated in figure 3. This single-phase alloy was heated to $1,280^\circ$ C for 1 hour and furnace-cooled.

X-Ray Diffraction Data

Extensive X-ray diffraction studies were made in this investigation to confirm the results observed during metallographic studies and to identify the phases present. The crystal structure of intermetallic compounds was also determined. Samples of alloys of 24 different compositions were studied. Most of these alloys were first studied using the same specimen and surface that was examined metallographically. The specimens were mounted in the rotating sample holder of a diffractometer. A molybdenum target X-ray tube was used with a zirconium filter and a krypton-filled Geiger tube. Those samples which were brittle enough to pulverize were reanalyzed as powders.

in the diffractometer to produce more nearly random orientation of crystallites. In those cases where even greater resolution seemed necessary, the samples were reanalyzed in a 114.6 mm-diameter powder camera with manganese-filtered iron radiation.

The seven intermediate phases, $\text{Ni}_{15}\text{Gd}_2$, Ni_5Gd , Ni_7Gd_2 , Ni_3Gd , Ni_2Gd , NiGd , and NiGd_3 , that were identified by metallography, were also identified by X-ray diffraction. These seven compounds are discussed individually as follows:

1. $\text{Ni}_{15}\text{Gd}_2$ was determined to crystallize in the hexagonal system, $a_o = 8.336$ Å, $c_o = 8.054$ Å. The X-ray pattern is tabulated in table 5. The observed atomic ratios and the lattice parameters of this compound were unlike those reported by Novy, Kleber, and Vickery (17) for the compound occurring in this composition range. They reported $\text{Ni}_{15}\text{Gd}_2$, hexagonal, $a_o = 8.18$ Å, and $c_o = 8.98$ Å. The atomic ratio of the compound also differed from that reported by Beaudry and Daane (2) in this composition range for nickel-yttrium alloys. They reported Ni_{17}Y_2 , hexagonal, $a_o = 8.34$ Å, $c_o = 8.08$ Å. These lattice parameters agreed very closely to those observed in this investigation, but metallographic studies did not confirm the same composition.

2. Ni_5Gd was found to have a hexagonal unit cell with $a_o = 4.902$ Å and $c_o = 3.964$ Å. This is substantially in agreement with the findings of Endter and Klemm (8) who reported $a_o = 4.91$ Å and $c_o = 3.99$ Å, and Nassau, Cherry, and Wallace (16) who reported $a_o = 4.90$ Å and $c_o = 3.96$ Å. The latter authors state that Ni_5Gd has the Cu_5Ca -type (also known as Zn_5Ca) structure along with 18 other compounds of the formula-type A_5B , where A represents the element alloyed to the rare earth B. The systematic extinctions observed for Ni_5Gd in this investigation can be attributed to space group $\text{P6}/\text{mmm}$, which is the space group of Cu_5Ca . The X-ray pattern observed for Ni_5Gd in this investigation is listed in table 6.

3. Ni_7Gd_2 was observed to have a hexagonal unit cell with $a_o = 4.960$ Å and $c_o = 2.422$ Å. The systematic extinctions appear to be consistent with the space group $\text{P6}_3/\text{mmc}$, which has been reported by Cromer and Larson (5) to be the probable space group of the analogous compound Ce_2Ni_7 . The similarity of these two unit cells makes it seem very probable that Ni_7Gd_2 is isostructural with Ni_7Ce_2 . This structure consists of double layers of the Ni_5Ce structure ($\text{Cu}_5\text{-Ca}$ -type) alternating with double layers of the Ni_2Ce structure (MgCu_2 -type). The X-ray data observed in the Bureau analysis of this compound are tabulated in table 7.

4. Ni_3Gd was determined to crystallize in the hexagonal system with $a_o = 4.982$ Å and $c_o = 16.31$ Å. Cromer and Olsen (6) reported that Ni_3Ce is hexagonal with similar parameters and the space group $\text{P6}_3/\text{mmc}$. Since the systematic extinctions observed for Ni_3Gd agree with those of that space group, it seems probable that Ni_3Gd is isostructural with Ni_3Ce . The X-ray data noted are listed in table 8.

TABLE 5. - $\text{Ni}_{15}\text{Gd}_2$ X-ray diffraction data¹

d (observed), angstroms	d (calculated), angstroms	Relative (observed) intensity	hkl planes
3.504	3.515	1	102
3.286	2.393	6	201
2.987	2.895	30	112
2.687	2.687	5	202
-	2.684	-	003
2.586	2.585	7	211
2.510	2.516	3	103
2.407	2.406	32	300
2.257	2.259	4	212
-	2.257	-	113
2.155	2.154	28	203
2.086	2.084	50	220
2.065	2.065	100	302
2.014	2.013	39	004
1.914	1.914	15	213
1.852	1.851	19	222
1.811	1.813	2	114
1.760	1.761	6	401
1.620	1.620	8	214
1.546	1.544	9	304
1.469	1.467	11	412
1.450	1.448	18	224
1.410	1.410	8	323
1.389	1.389	8	330
1.313	1.313	10	322
1.278	1.279	8	324
-	1.278	-	116
1.216	1.216	5	423
1.203	1.203	10	600
1.172	1.172	13	306
1.154	1.155	3	325
1.129	1.129	1	424
1.111	1.111	2	522
1.0939	1.096	1	207
-	1.091	-	611
1.075	1.075	1	505
1.042	1.042	12	440
1.033	1.033	8	441
1.022	1.022	9	434
-	1.021	-	416
1.010	1.010	2	515

¹Crystal system: hexagonal.Lattice constants: $a_o = 8.336 \text{ \AA}$, $c_o = 8.054 \text{ \AA}$.

TABLE 6. - Ni_5Gd X-ray diffraction data¹

d (observed), angstroms	d (calculated), angstroms	Relative (observed) intensity	hkl planes
3.969	3.963	8	001
2.895	2.899	45	101
2.451	2.454	20	110
2.125	2.125	30	200
2.086	2.086	100	111
1.981	1.982	40	002
1.874	1.873	10	201
1.543	1.542	13	112
1.490	1.489	13	211
1.450	1.450	30	202
1.417	1.417	6	300
1.334	1.334	27	301
1.261	1.262	6	103
1.227	1.227	11	220
1.163	1.163	24	113
1.153	1.153	10	302
1.130	1.130	7	313
1.063	1.063	3	400
1.043	1.043	18	222
1.020	1.020	6	213
.991	.991	5	004

¹Crystal system: hexagonal.Space group: $P6/mmm$.Lattice constants: $a_0 = 4.902$ A, $c_0 = 3.964$ A.

5. Ni_2Gd was determined to be a cubic MgCu_2 , Laves-type phase, with a $Fd3m$ space group and $a_0 = 7.223$ A. The X-ray diffraction data are presented in table 9. Novy, Kleber, and Vickery (17) reported a parameter measurement of $a_0 = 7.27$ A. Many other compounds of the stoichiometric ratio of A_2B , where A represents the elements alloyed to rare earth B, are reported in the literature to have the MgCu_2 -type structure.

6. NiGd : When a sample of NiGd was broken up to prepare a powder sample, one of the pieces was found to be a single crystal. This crystal was studied on a Buerger Precession camera and was found to be orthorhombic with $a_0 = 3.765$ A, $b_0 = 10.30$ A, and $c_0 = 4.24$ A. The X-ray data observed are in table 10. The systematic extinctions were those of space groups Cmcm , $\text{Cmc}2_1$, and C_2cm . This unit cell closely resembles that reported by Finney and Rosenzweig (9) for the analogous compound NiCe which is orthorhombic $a_0 = 3.88$ A, $b_0 = 10.46$ A, and $c_0 = 4.37$ A, space group Cmcm . They show that NiCe has the ThI (also known as CrB) type of structure. It seems likely that NiGd has this structure, but further work will be necessary to prove this definitely. The sample studied in this investigation definitely does not have the FeB structure reported for NiGd by Baenziger and Moriarty (1).

TABLE 7. - Ni_7Gd_2 X-ray diffraction data¹

d (observed), angstroms	d (calculated), angstroms	Relative (observed) intensity	hkl planes
4.280	4.295	3	100
4.025	4.036	5	006
3.027	3.028	4	008
2.740	-	15	-
2.697	2.695	20	107
2.478	2.470	40	110
2.143	2.147	40	200
-	2.140	-	201
2.108	2.115	100	202
-	2.113	-	116
-	2.109	-	1, 0, 10
2.012	2.018	25	0012
1.963	1.963	15	205
-	1.959	-	1, 0, 11
1.918	1.918	3	118
1.787	-	3	-
1.732	1.730	10	0014
1.565	1.565	2	1, 1, 12
1.542	1.539	2	215
1.514	1.514	2	0016
1.473	1.471	10	2, 0, 12
-	1.470	-	212
1.432	1.432	15	300
1.419	1.419	10	1, 1, 14
1.348	1.346	18	0018
1.295	1.294	4	308
1.240	1.240	18	220
1.210	1.211	3	0020
1.183	1.184	5	2, 1, 14
-	1.183	-	226
1.129	1.127	5	317
1.117	1.114	3	1, 0, 21
1.105	1.104	5	2, 2, 10
1.090	1.089	5	319
1.073	1.074	5	400
1.057	1.057	5	404
1.009	1.009	10	0024

¹Crystal system: hexagonal.Space group: $P6_3/mmc$.Lattice constants: $a_0 = 4.960$ Å, $c_0 = 2.422$ Å.

TABLE 8. - Ni_3Gd X-ray diffraction data¹

d (observed), angstroms	d (calculated), angstroms	Relative (observed) intensity	hkl planes
4.280	4.315	5	100
4.110	4.076	7	004
2.775	-	10	-
2.715	2.718	65	006
2.617	2.606	3	105
2.491	2.491	80	110
2.168	2.158	30	200
2.135	2.139	100	201
2.110	2.126	80	114
2.041	2.050	40	107
-	2.038	-	008
2.015	2.006	40	203
1.978	1.980	33	115
1.840	1.843	15	108
-	1.837	-	116
1.628	1.631	14	0, 0, 10
-	-	-	210
1.485	1.483	15	0011
-	1.482	-	208
1.442	1.438	22	300
1.419	1.417	20	302
1.367	1.364	10	1, 1, 10
1.359	1.359	40	0012
1.350	1.354	20	304
1.319	1.314	6	305
1.246	1.246	13	220
1.240	1.242	10	221
1.133	1.132	5	226
1.098	1.098	5	227
1.080	1.079	10	400
1.064	1.064	5	317
1.056	1.054	12	1, 0, 15
.991	.990	5	320

¹Crystal system: hexagonal.Space group: $P6_3/mmc$.Lattice constants: $a_0 = 4.982 \text{ \AA}$, $c_0 = 16.31 \text{ \AA}$.

TABLE 9. - Ni_2Gd X-ray diffraction data¹

d (observed), angstroms	d (calculated), angstroms	Relative (observed) intensity	hkl planes
4.200	4.170	10	111
2.560	2.560	80	220
2.180	2.180	100	311
2.090	2.090	30	222
1.660	1.660	5	331
1.480	1.480	40	422
1.390	1.390	45	511
-	-	-	333
1.279	1.277	45	440
1.143	1.142	15	620
1.102	1.101	19	533
1.089	1.089	10	622
.9655	.9652	13	642
.9406	.9404	22	731
.9020	.9029	3	800
.8503	.8512	5	822
-	-	-	660
.8337	.8340	11	751
-	-	-	555
.7934	.7928	2	911
-	-	-	753
.7706	.7700	2	664
.7566	.7572	5	931
.7373	.7372	9	844

¹Crystal system: cubic.Space group: $\text{Fd}\bar{3}\text{m}$.Lattice constant: $a_0 = 7.223 \text{ \AA}$.

7. NiGd_3 's unit cell is unknown, for repeated attempts to index the pattern were unsuccessful. There is also some uncertainty about a few diffraction lines in the pattern since some of them may be caused by the presence of small amounts of other phases. However, there are enough lines which cannot be attributed to any other compound so that there can be little doubt that such a compound exists. The X-ray data observed are tabulated in table 11.

TABLE 10. - NiGd X-ray diffraction data¹

d (observed), angstroms	d (calculated), angstroms	Relative (observed) intensity	hkl planes
3.317	-	5	-
3.251	3.273	25	021
3.115	-	<5	-
3.092	-	5	-
2.704	2.706	75	111
2.635	-	5	-
2.561	2.575	100	040
2.193	2.201	40	041
2.176	2.172	45	311
2.114	2.120	50	002
1.875	1.869	5	200
1.655	1.660	15	151
1.626	1.623	30	221
-	1.625	-	132
1.592	1.591	15	061
1.517	1.512	5	240
1.469	-	<5	-
1.421	1.425	5	241
1.368	1.369	15	170
1.307	1.311	10	113
1.267	1.264	<5	260
1.231	1.232	15	081
-	1.231	-	242
1.213	1.212	5	261
1.148	1.150	10	172
1.112	1.106	<5	153
1.098	1.101	25	223
1.089	-	<5	-
1.055	1.060	5	004
1.027	1.030	5	0, 10, 0
-	1.025	-	332
.999	1.001	<5	0, 10, 1

¹Crystal system: orthorhombic.

Space group: probably Cmcm.

Lattice constants: $a_0 = 3.765$ A, $b_0 = 10.30$ A, $c_0 = 4.24$ A.

TABLE 11. - NiGd_3 X-ray diffraction data

d (observed), angstroms	Relative (observed) intensity	d (observed), angstroms	Relative (observed) intensity
3.344	10	1.798	8
3.238	10	1.741	5
3.139	10	1.706	15
3.023	13	1.661	21
2.885	-	1.626	12
2.865	100	1.610	37
2.816	27	1.553	36
2.750	37	1.542	40
2.696	9	1.519	35
2.635	30	1.481	20
2.594	5	1.436	15
2.561	45	1.393	21
2.462	21	1.370	20
2.404	8	1.344	7
2.349	16	1.323	6
2.265	9	1.298	12
2.164	22	1.291	10
2.104	13	-	-
1.978	9	-	-
1.854	20	-	-

DISCUSSION OF RESULTS

The identification of all of the intermetallic compounds was difficult when as-cast alloys were used for metallographic studies. Cored structures masked the presence of several of the compounds, notably in the composition range where Ni_7Gd_2 , Ni_3Gd , and Ni_2Gd occurred. For this reason all the alloys were made homogeneous by annealing treatments before analyses by thermal, metallographic, or X-ray diffraction techniques.

Metallographic and thermal analysis data, indicating the presence of a solidus boundary, correlated well, usually with a variation of less than 10°C . Metallographic data were used to substantiate the temperature and the composition extent of all peritectic and eutectic isotherms as indicated by thermal analyses. Whenever a confliction of thermal analyses and metallographic data was observed, the latter was used to determine the extent of the isotherm. The structures resulting from heating several alloy compositions to temperatures slightly exceeding their respective solidus isotherms are illustrated in figures 4 through 9. A sample containing 10 percent gadolinium heated to 20°C above the eutectic isotherm occurring at $1,290^\circ\text{C}$ is illustrated in figure 4. A eutectic structure and nickel are depicted in this illustration. The structure of four heat-treated specimens, which helped place the location of the peritectic isotherms where $\text{Ni}_{15}\text{Gd}_2$, Ni_7Gd_2 , Ni_3Gd , and Ni_2Gd melt incongruently, are illustrated in figures 5, 6, 7, and 8, respectively. The eutectic structure resulting from heating a Ni-70 percent Gd alloy 10°C above the eutectic isotherm occurring at 890°C is illustrated in figure 9.

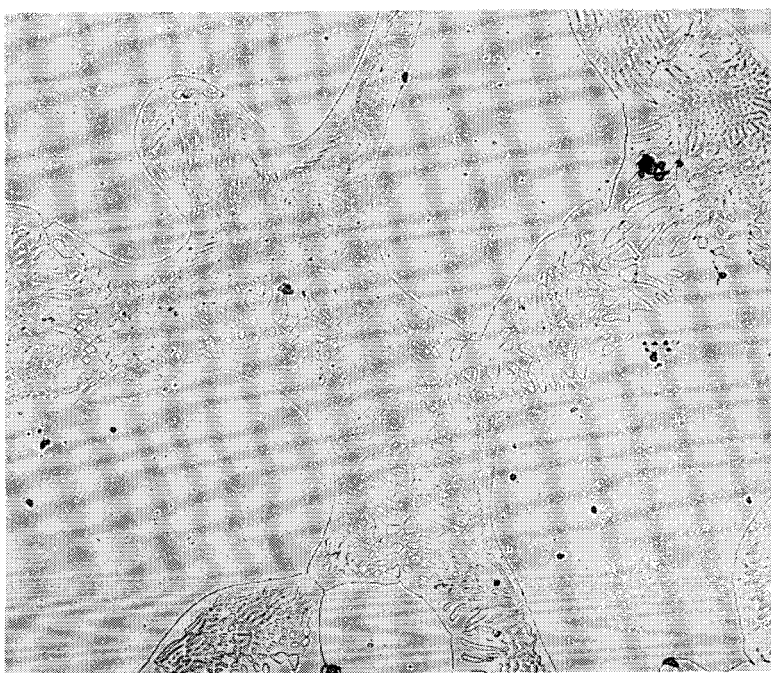
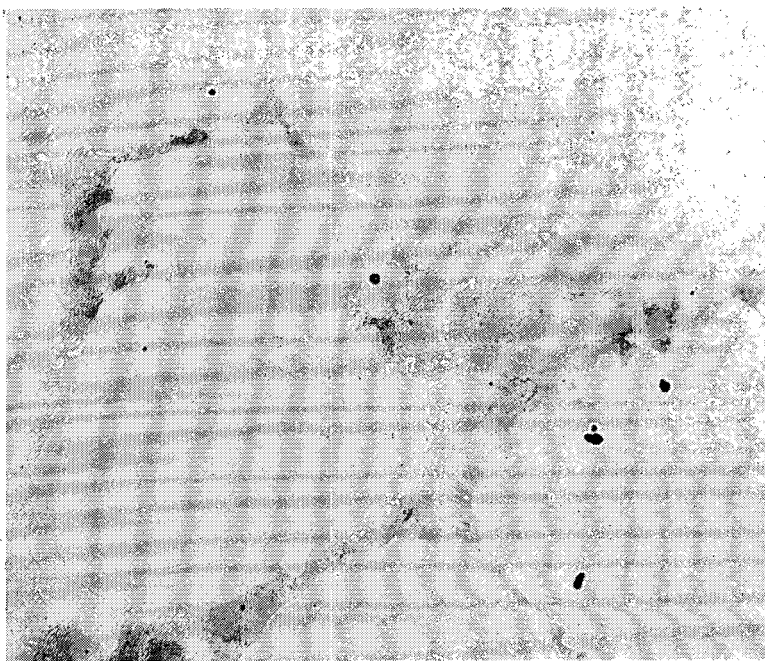


FIGURE 4. - Dendritic Structure Observed in an Ni-10 wt pct Gd Alloy (X 500); Chromic Acid Etch.

FIGURE 5. - Cored Structure in Ni-26.4 wt pct Gd Specimen Developed After Heat Treatment at 1310°C (X 500); Chromic Acid Etch.



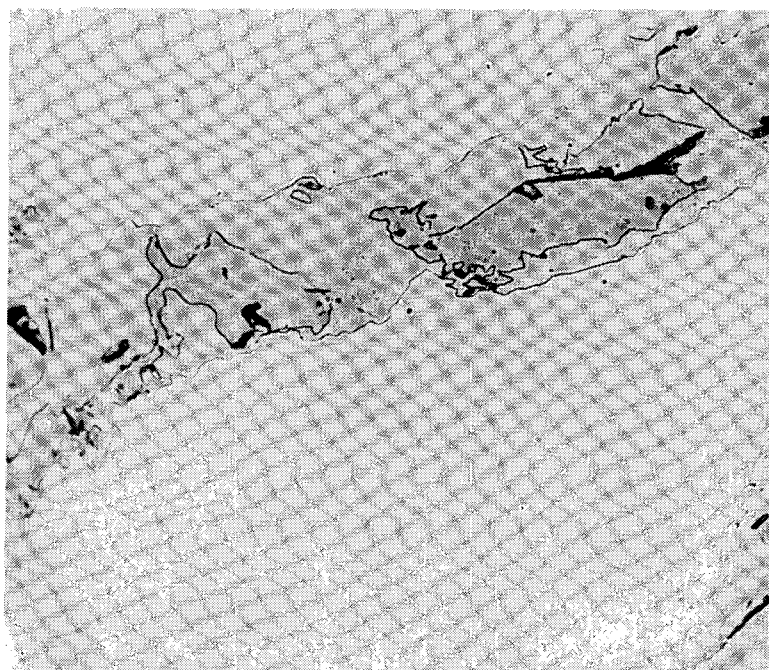


FIGURE 6. - Structure of an Ni-37.5 wt pct Gd Alloy Held at 10°C Above the Peritectic Isotherm Occurring at 1,270°C (X 500); Nital Etch.

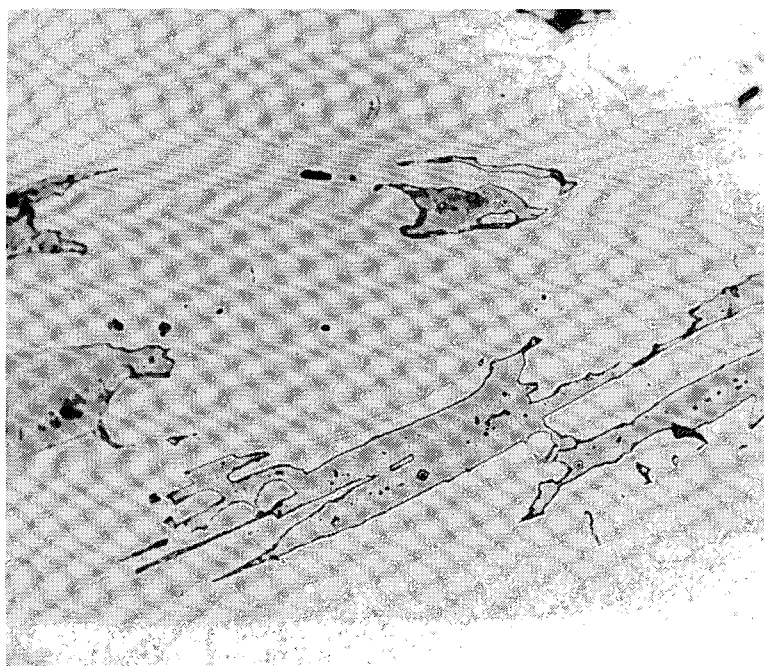


FIGURE 7. - Cored Structure in an Ni-45 wt pct Gd Alloy After Heat Treatment at 10° C Above the Peritectic Isotherm Occurring at 1,180°C (X 500); Nital Etch.

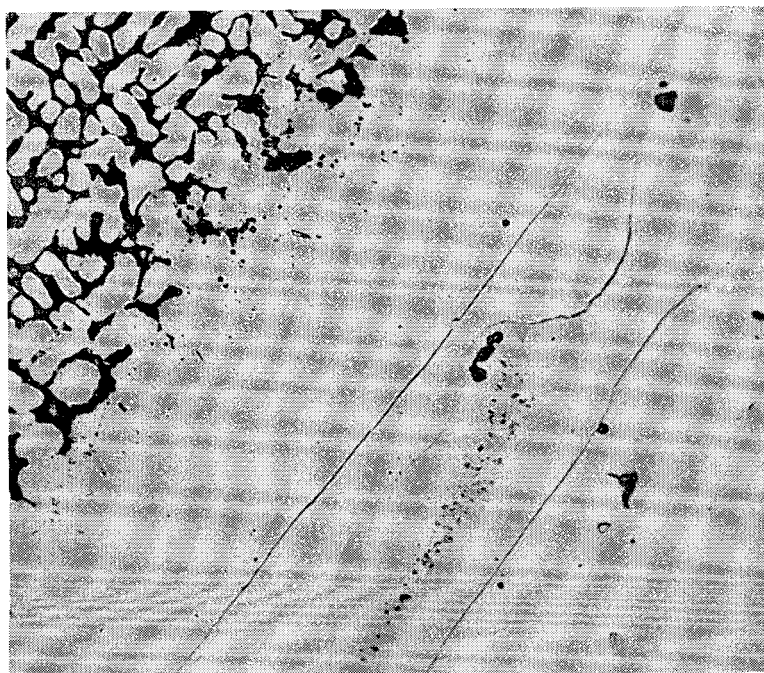


FIGURE 8. - Cored Structure Observed After Holding at 10°C Above the Peritectic Isotherm at $1,070^{\circ}\text{C}$, Where Ni_2Gd Melted Incongruently (X500); Nital Etch.

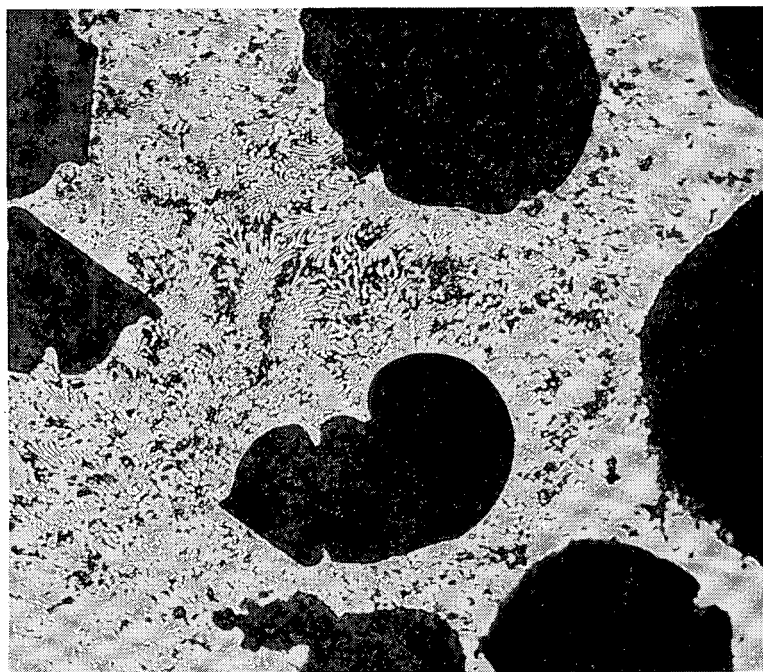


FIGURE 9. - Eutectic Structure Observed in an Ni-70 wt pct Gd Specimen Held at 10°C Above the 890°C Isotherm (X500); Nital Etch.

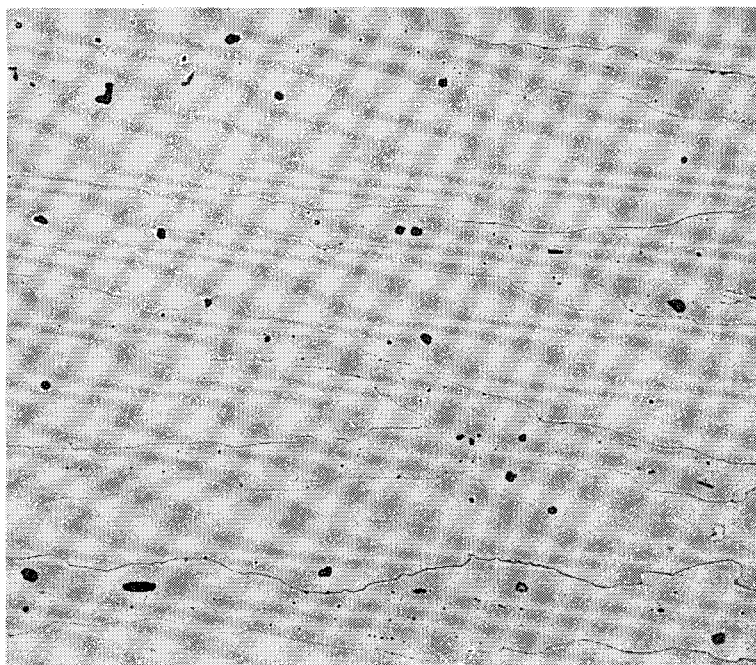


FIGURE 10. - Duplex Structure Consisting of Ni_5Gd and Ni_7Gd_2 Observed in an Annealed Ni-39 wt pct Gd Specimen (X 500); Nital Etch.

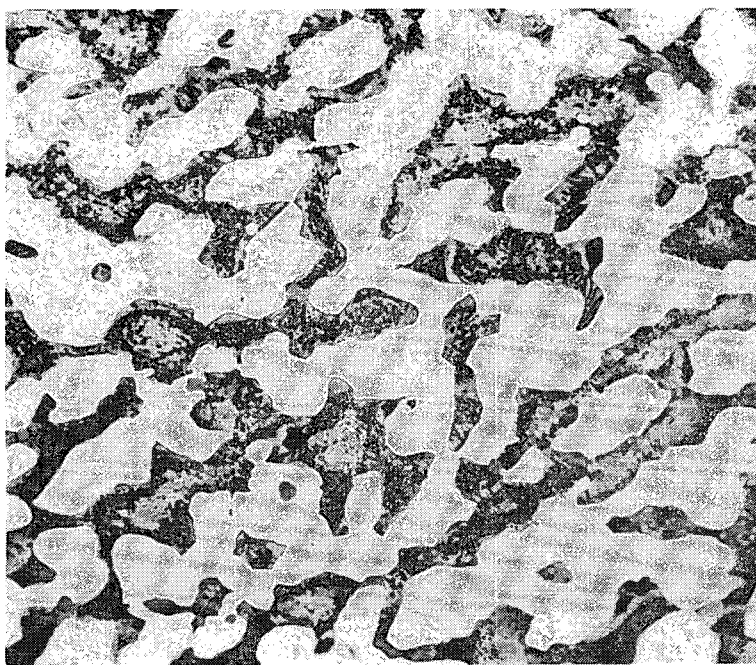


FIGURE 11. - NiGd and NiGd_3 Phases Observed in an Ni-80 wt pct Gd Alloy (X 500); Nital Etch.

The solid solubility of the phases in each other were determined metallographically. No solid solubility of the phases in each other was observed except for a small solubility of $\text{Ni}_{15}\text{Gd}_2$ in Ni_5Gd . All of the intermetallic phases, except Ni_5Gd , were of constant stoichiometric composition.

The effect of nickel on the gadolinium transformation occurring at $1,264^\circ\text{C}$ was not investigated. An extensive solid plus liquid phase region was observed to occur at temperatures much below the transformation. This factor plus the very limited solid solubility of NiGd_3 in gadolinium indicated that very little change would be expected in the transformation of gadolinium on alloying with nickel.

Two of the compounds, Ni_4Gd and Ni_2Gd_3 , reported by Novy, Kleber, and Vickery (17), were not observed in this investigation. A structure containing the phases Ni_5Gd and Ni_7Gd_2 is illustrated in figure 10. This alloy, whose composition was isotypic with the compound Ni_4Gd containing 39-wt pct gadolinium, was annealed at $1,100^\circ\text{C}$ for 2 days. A specimen containing almost equal parts of NiGd and NiGd_3 , observed in an alloy containing 80-wt pct gadolinium after annealing at 690°C , is illustrated in figure 11. This alloy composition would be isotypic with Ni_2Gd_3 .

CONCLUSIONS

The nickel-gadolinium phase diagram illustrated in figures 1 and 2 was believed accurate within 10°C in temperature and 2 percent in composition. The alloy system contains three eutectics and seven compounds. The eutectics occur at 13, 67, and 85 percent gadolinium, and they melt at $1,290^\circ$, 890° , and 700°C , respectively. The compounds observed are $\text{Ni}_{15}\text{Gd}_2$, Ni_5Gd , Ni_7Gd_2 , Ni_3Gd , Ni_2Gd , NiGd , and NiGd_3 ; the first four crystallize in the hexagonal system. Ni_2Gd is a Laves phase with a cubic structure. NiGd crystallizes in the orthorhombic system, and the crystal system of NiGd_3 was not identified. The five observed phases, $\text{Ni}_{15}\text{Gd}_2$, Ni_7Gd_2 , Ni_3Gd , Ni_2Gd , and NiGd_3 , melt peritectically at $1,300^\circ$, $1,270^\circ$, $1,180^\circ$, $1,070^\circ$, and 775°C , respectively. Ni_5Gd and NiGd melt congruently at $1,550^\circ$ and 980°C , respectively. Very little solid solubility of the phases in each other was observed except for a slight solubility of $\text{Ni}_{15}\text{Gd}_2$ in Ni_5Gd . The effect of nickel on the transformation temperature of gadolinium was not investigated.

REFERENCES

1. Baenziger, N. C., and J. L. Moriarty, Jr. Gadolinium and Dysprosium Intermetallic Phases. The Crystal Structures of DyGa and GdPt and Their Related Compounds. *Acta Cryst.*, v. 14, 1961, p. 946.
2. Beaudry, B., and A. H. Daane. Yttrium-Nickel System. *Trans. AIME*, v. 218 *Met. Soc.*, 1960, pp. 854-859.
3. Copeland, M., and H. Kato. Gadolinium Alloys of Iron, Chromium, Nickel, and Stainless Steel in Rare Earth Research, edited by J. Nochman and C. Lundin, Gordon and Breach Science Publishers, N.Y., 1962, pp. 133-143.
4. Copeland, M. I., M. Krug, C. E. Armantrout, and H. Kato. Iron-Gadolinium Phase Diagram. *BuMines Rept. of Inv.* 5925, 1962, 16 pp.
5. Cromer, D. T., and A. C. Larson. The Structure of Ni_7Ce_2 . *Acta Cryst.*, v. 12, 1959, pp. 855-858.
6. Cromer, D. T., and C. E. Olsen. The Crystal Structures of $PuNi_3$ and $CeNi_3$. *Acta Cryst.*, v. 12, 1959, pp. 689-694.
7. Deardorff, D. K., and E. T. Hayes. Melting-Point Determination of Hafnium, Zirconium, and Titanium. *J. Metals*, v. 8, No. 5, May 1956, pp. 509-511.
8. Endter, F., and W. Klemm. Structure of Ni_5Gd . *Ztschr. Anorg. All. Chem.* (Journal for Inorganic and General Chemistry), v. 252, 1943, pp. 64-66.
9. Finney, J. J., and A. Rosenzweig. The Structure of $CeNi$. *Acta Cryst.*, v. 14, 1961, p. 69.
10. Gschneidner, K. A., Jr., and James Weber. Principles of Alloying Behavior of Rare Earth Metals. Los Alamos Scientific Laboratory, Los Alamos, N. Mex., undated, 71 pp.
11. Hansen, M. Constitution of Binary Alloys. McGraw-Hill Book Co., Inc., New York, 1958, pp. 525-533, 541-546, 677-684.
12. Howes, R. B. The Rare Earths. *Metals Prog.*, v. 75, No. 6, June 1959, pp. 108-112.
13. Hughes, D. J., and J. A. Harvey. Neutron Cross Sections. Brookhaven National Laboratory, Upton, N.Y., BNL 325, July 1, 1955, pp. 8, 18.
14. Hume-Rothery, W. Structure of Metals and Alloys. Institute of Metals, London, 1954, 363 pp.

15. Moriarty, J., and N. Baenziger. Rare Earth Phase Diagrams. Rare Earth Symposium, Am. Soc. Metals, Chicago, Ill., November 1959.
16. Nassau, K., L. V. Cherry, and W. E. Wallace. Intermetallic Compounds Between Lanthanous and Transition Metals of the First Long Periods. J. Phys. Chem. Solids, v. 16, 1960, pp. 123-130.
17. Novy, V. F., E. V. Kleber, and R. C. Vickery. The Gadolinium-Nickel System. Trans. AIME, v. 221 (Met. Soc.), 1961, pp. 585-588.
18. Taylor, L. The Metals Handbook. American Society for Metals, Cleveland, Ohio, 8th ed., 1961, pp. 44-51.
19. Teatum, E., K. Gschneidner, Jr., and J. Weber. Compilation of Calculated Data Useful in Predicting Metallurgical Behaviors of the Elements in Binary Alloy Systems. Los Alamos Scientific Laboratory, Los Alamos, N. Mex., LA-2345, June 1960, 225 pp.
20. Wernick, J. H., and E. Geller. Transition Element-Rare Earth Compounds With Ca_5Ca Structure. Acta Cryst., v. 12, 1959, pp. 662-665.